RSC Advances

PAPER

View Article Online
View Journal | View Issue

Cite this: *RSC Adv.*, 2017, **7**, 18893

Discovery of phosphorodiamidate mustard-based O^2-phosphorylated diazeniumdiolates with potent anticancer activity†

Yu Zou,[a] Chang Yan,[a] Edward E. Knaus,[b] Huibin Zhang,*[a] Yihua Zhang*[a] and Zhangjian Huang *[a]

Nitric oxide (NO) has recently joined the clinical arena of cancer therapy because high levels of NO could not only induce cytotoxicity and apoptosis of cancer cells, but also sensitize the cells to chemo- and radiotherapies. Diazeniumdiolates are an important class of NO donors, and the O^2-alkylation, arylation and sulfonylation of diazeniumdiolates result in more stable and potent anticancer agents. However, O^2-phosphorylation has so far not been reported yet. Herein, we describe the design, synthesis and biological evaluation of a group of phosphorodiamidate mustard-based O^2-phosphorylated diazeniumdiolates, **6–9**. The most active compound, **7**, was comparable, or even more potent, than a known anticancer agent, O^2-2,4-dinitrobenzene diazeniumdiolate JS-K, against six cancer cell lines. Furthermore, **7** released larger amounts of NO, caused more significant DNA damage and cancer cell apoptosis than JS-K in the cancer cells. Our findings suggest that this new type of O^2-substituted diazeniumdiolate could be potentially applied in the fight against cancer.

Received 10th January 2017
Accepted 21st March 2017

DOI: 10.1039/c7ra00401j

rsc.li/rsc-advances

Introduction

Nitric oxide (NO) is known to mediate numerous physiological processes, including vasodilation, neurotransmission and immune response.[1] Currently, it has become clear that high levels of NO can damage biomacromolecules such as proteins, DNA and lipids, and cause cell death by triggering apoptosis.[2] Additionally, NO is capable of interacting with reactive oxygen species (ROS) to form a variety of highly reactive nitrogen oxides (NOx), involving peroxynitrite anion ($ONOO^-$), nitrogen dioxide (NO_2), and dinitrogen trioxide (N_2O_3), *etc.* which are responsible for cytotoxic nitration and nitrosylation.[3–5] Therefore, NO is considered as a potential anticancer agent and has joined the clinical arena of cancer therapy.[6–8] Since NO is implicated in a myriad of biological processes, however, NO donor compounds should release large amounts of NO localized at cancer sites in order to exert anticancer activity and avoid side effects.

Diazeniumdiolates are an important class of NO donors, which spontaneously release two molecules of NO under physiological conditions (pH 7.4, 37 °C) with a range of half-lives from a few seconds to several hours.[9] To enhance their stability and selectivity, a large number of O^2-derived diazeniumdiolates have been synthesized (Fig. 1), and these derivatives can be enzymatically cleaved to produce NO. For instance, O^2-carbonyloxymethylated (**1**), O^2-glycosylated diazeniumdiolates (**2**), and O^2-arylated (JS-K, **3**) could be selectively triggered by esterases,[10] glycosidases,[11] and glutathione/glutathione S-transferases,[12–14] respectively, to generate diazeniumdiolate anion, which spontaneously liberate NO *in situ* exhibiting potent biological activity. Among them, JS-K displayed significant anticancer activity in a broad spectrum of human cancer cell lines *in vitro* as well as in several mouse xenograft models *in vivo*.[15]

O^2-Derived diazeniumdiolates (Fig. 1) are generally synthesized by O^2-alkylation (for **1** and **2**), arylation (for **3**) or

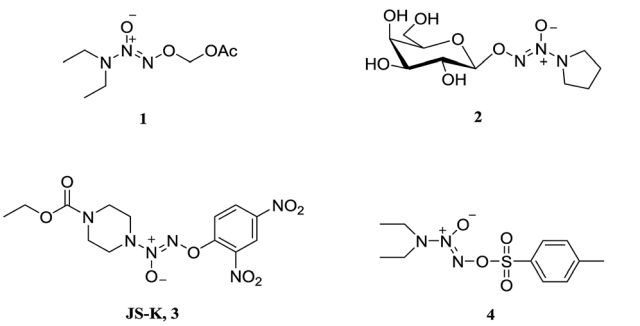

Fig. 1 Structures of some important O^2-derived diazeniumdiolates.

[a]State Key Laboratory of Natural Medicines, Jiangsu Key Laboratory of Drug Discovery for Metabolic Diseases, Jiangsu Key Laboratory of Drug Screening, China Pharmaceutical University, Nanjing 210009, PR China. E-mail: zhangjianhuang@cpu.edu.cn; zyhtgd@163.com; zhanghb80@163.com

[b]Faculty of Pharmacy and Pharmaceutical Sciences, University of Alberta, Edmonton, Alberta T6G 2E1, Canada

† Electronic supplementary information (ESI) available: The synthetic route for compound **5**; experimental procedures for **5**, **10**, **11** and **12**; ^{1}H NMR, ^{13}C NMR, ^{31}P NMR and HRMS spectra of **6–9**. See DOI: 10.1039/c7ra00401j

sulfonylation (for **4**).[16] As far as we know, O^2-phosphorylation has not yet been documented. It was therefore of interest to examine whether O^2-phosphorylation of diazeniumdiolates could be achieved and exert anticancer activity.

In this article, we would like to report the design, synthesis and biological evaluation of O^2-phosphorylated diazeniumdiolates.

Results and discussion

Rationale for the design of O^2-phosphorylated diazeniumdiolates

We initially investigated the reaction of 1-(*N*,*N*-diethylamino) diazen-1-ium-1,2-diolate sodium with bis(dimethyl-amino) phosphoryl chloride, that could afford O^2-phosphorylated diazeniumdiolate **5** (Scheme S1 in ESI†). Based on this success, it was therefore of interest to extend the scope of O^2-phosphorylated diazeniumdiolate derivatives using various substituted phosphoryl chlorides.

It is known that phosphoramide and phosphorodiamidate mustards are cytotoxins, which can be produced from enzymatic activation of some known anticancer drugs. For example, *N*,*N*,*N*′,*N*′-tetrakis(2-chloroethyl)phosphorodiamidic acid is derived from the glutathione S-transferase π (GSTπ) activation of canfosfamide (Fig. 2A) *via* a Tyr 7 triggered deprotonation and β-elimination cleavage.[17] In this context, we hypothesized that phosphorodiamidate mustard-based O^2-phosphorylated diazeniumdiolates might produce phosphorodiamidate mustard and diazeniumdiolate moieties after *in vivo* metabolism, exerting significant anticancer activity (Fig. 2B).

Chemistry

To verify the above hypothesis, we synthesized phosphorodiamidate mustard-based O^2-phosphorylated diazeniumdiolates **6–9** as depicted in Scheme 1. Compound **10** was prepared by the reaction of phosphorous oxychloride with nitrogen mustard hydrochloride in toluene in the presence of triethylamine at room temperature, then treatment of **10** with another molecule of nitrogen mustard hydrochloride under the same conditions

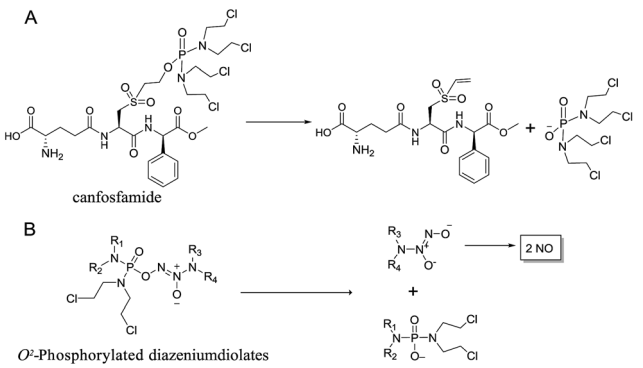

Fig. 2 (A) Activation of canfosfamide to form phosphoro-diamidate mustard. (B) Rationale for the design of phosphorodiamidate mustard-based O^2-phosphorylated diazeniumdiolates and the proposed mechanism of action.

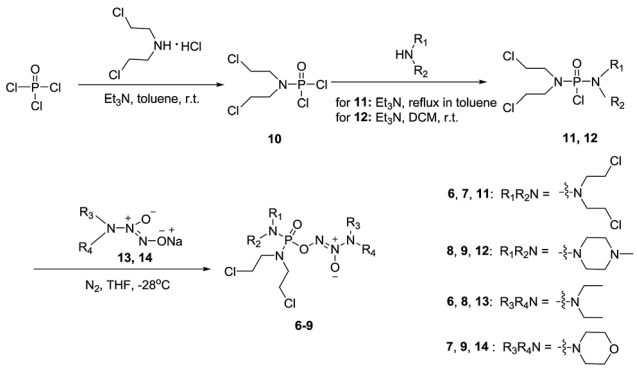

Scheme 1 The synthetic route for target compounds **6–9**.

except that reaction temperature was raised to 110 °C, yielding phosphorodiamidate mustard **11**.

Compound **12** was obtained by reaction of **10** with *N*-methyl piperazine in dichloromethane in the presence of triethylamine at room temperature. On the other hand, the corresponding secondary amines were treated with NO gas (50 psi) in the presence of NaOMe, forming diazeniumdiolate sodium salts **13**

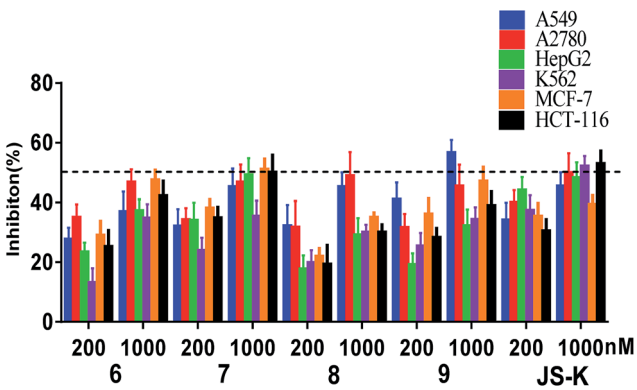

Fig. 3 Inhibitory activity of **6–9** at 200 nM and 1000 nM against cancer A549, A2780, HepG2, K562, MCF-7 and HCT-116 cells after incubation for 72 h. Cell proliferation was determined by MTT assay. Data are means ± SD of the inhibition (%) from three independent experiments.

Table 1 IC_{50} values (μM) of **7** and JS-K against HCT-116, A549, A2780, HepG2, MCF-7 and MCF10A cells[a]

	7	JS-K
HCT-116	0.847 ± 0.09	0.698 ± 0.08
A549	1.56 ± 0.21	1.53 ± 0.18
A2780	1.27 ± 0.10	1.59 ± 0.16
HepG2	1.29 ± 0.09	1.00 ± 0.12
MCF-7	0.651 ± 0.07[b]	1.60 ± 0.19
MCF10A	86.5 ± 15.5	23.5 ± 4.52

[a] The IC_{50}s of **7** and JS-K against several cancer cells and normal breast epithelial MCF10A cells were determined by MTT assay. Data were expressed as the means ± SD of each group of cells from five individual experiments. Without other mentioned, the incubation time is 72 h. [b] The IC_{50}s of **7** against MCF-7 during 24 or 48 h incubation periods are 1.78 ± 0.13 μM or 1.26 ± 0.11 μM, respectively.

and **14**.[9] Finally, condensation of **11** and **12** with **13** and **14** in tetrahydrofuran under the nitrogen protection at −28 °C furnished **6–9**, respectively.

Assessment of *in vitro* anti-proliferative activity

Compounds **6–9** were tested for their anti-proliferative activity against six human cancer cell lines (A549, A2780, HepG2, K562, MCF-7 and HCT-116) by MTT assay using JS-K as a positive control (Fig. 3).

As shown in Fig. 3, the most active compound **7** exhibited significant cytotoxicity on six human cancer cell lines, comparable to JS-K. Thus, we further determined the IC_{50} values of **7** as shown in Table 1. Evidently, **7** inhibited the proliferation of A549, A2780, HepG2, K562, and HT-29 cell lines as potent as JS-K and more potent against MCF-7 cells than JS-K. Interestingly, **7** exhibited much less antiproliferative activity against normal breast epithelial MCF10A cells (IC_{50} = 86.5 μM) than breast cancer MCF-7 cells (IC_{50} = 0.65 μM), suggesting the selective inhibition of compound **7** against cancer cells. Furthermore, the IC_{50}s of **7** against MCF-7 during 24, 48 or 72 h incubation periods were determined as 1.78, 1.26 or 0.65 μM (Table 1), respectively, suggesting that **7** exerted activity in a time-dependent manner.

Since compound **7** exhibited remarkable inhibitory activity against different cancer cells, especially for MCF-7 cell lines. MCF-7 cells were thus selected for further assays, including NO release, comet assay and apoptosis induction assay.

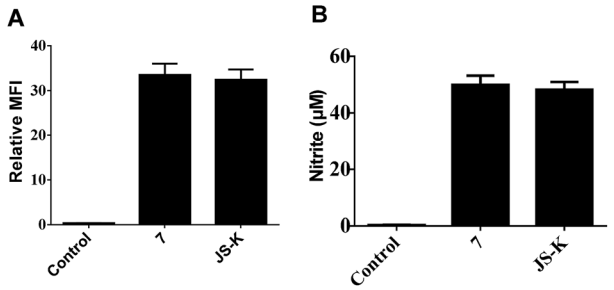

Fig. 4 Intracellular NO release behaviour of indicated compounds. (A) Quantitative measurement of intracellular NO production. MCF-7 cells were treated with indicated compounds (30 μM) for 6 h, and NO were measured as DAF-NO derivative fluorescence intensities (% of control). Data are expressed as means ± SD from three separate experiments. (B) MCF-7 cells were incubated with the indicated compounds (30 μM) for 24 h and the levels of NO (presented as nitrite) were determined using a colorimetric Griess reaction assay. Data are expressed as means ± SD from three separate experiments.

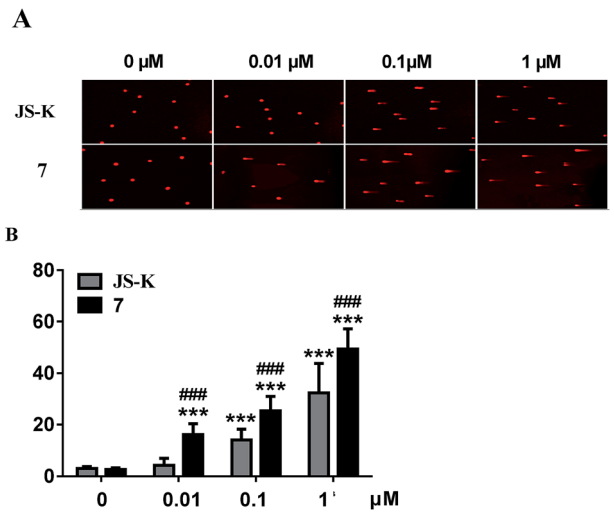

Fig. 5 Effect of compounds **7** and JS-K on MCF-7 cell DNA damage. MCF-7 cells were treated for 2 h in the presence or absence of **7** and JS-K (0.01, 0.1, 1 μM). (A) The cells were collected and alkaline comet electrophoresis were performed. (B) The quantitative analysis was performed with the comet analysis software CASP, and the olive tail moment was employed to evaluate DNA damage in **7** and JS-K treated MCF-7 cells. Assays were repeated three times and data were expressed as means ± SD. ***p < 0.001, *vs.* control, ###p < 0.001, *vs.* the same concentration of JS-K.

Assay of intracellular NO release

NO release behavior of **7** and JS-K in MCF-7 cells was examined using both NO-sensitive fluorophore, 4-amino-5-(methylamino)-2′,7′-difluorofluorescein diacetate (DAF-FM DA),[18] and Griess reagent.[19] It was observed that **7** showed more significant fluorescence (Fig. 4A) and produced greater amounts of nitrite

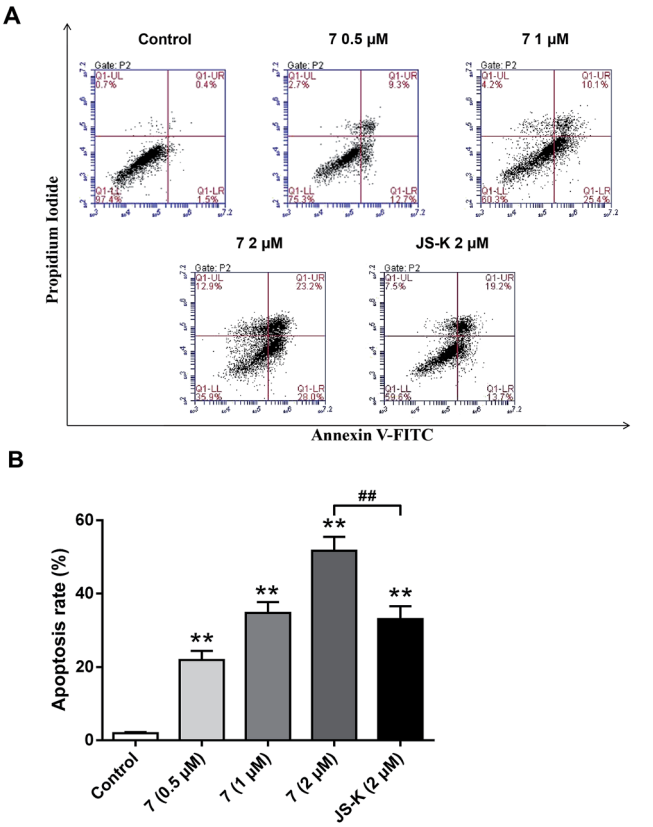

Fig. 6 Apoptosis of MCF-7 cells treated with the indicated concentrations of **7** for 24 hours. (A) Annexin V–FITC and propidium iodide (PI) staining were carried out. (B) The apoptosis rate was measured using flow cytometry. The percentage of cells in each population are shown as the means ± SD (n = 3). **P < 0.01, with control group; ##P < 0.01. The data are shown representative of three independent experiments.

(Fig. 4B), an oxidant product of NO, in MCF-7 cells than JS-K, indicating 7 released a larger amounts of NO than JS-K in MCF-7 cells.

Comet assay

Subsequently, DNA interstrand crosslink (ICL) activity of 7 and JS-K in the MCF-7 cells was tested using a well-established alkaline comet assay to examine cellular DNA damage. As visually shown in Fig. 5, 7 exhibited significant DNA ICL activity in a dose-dependent manner, and an obvious cellular DNA damage was observed as comet tails at 0.01 μM. In comparison, JS-K showed much lower DNA damage activity than 7, and no obvious cellular DNA damage was found under the same conditions. These results suggest that diazeniumdiolate together with the phosphoramide mustard moiety may display potent effects, making 7 more active in inducing DNA damage than JS-K.

Induction of MCF-7 cell apoptosis

To examine whether the inhibitory effects of 7 on breast cancer cellular proliferation are accompanied by enhanced cancer cell apoptosis, Annexin V–FITC and propidium iodide (PI) staining were carried out and the percentages of apoptotic cells were determined using flow cytometry assay. MCF-7 cells were incubated with different concentrations of vehicle, 7, or JS-K for 24 h. It was observed that treatment with 7 significantly induced apoptosis in MCF-7 cells, more potently than treatment with JS-K (Fig. 6).

Conclusion

The potential use of NO-donating drugs in anticancer field has drawn dramatic attention, and a large number of cancer cell lines have been proved to be sensitive to NO-induced cytotoxic effects.[20] It is of great importance to develop new O^2-substituted diazeniumdiolates and to extend the NO-based anticancer therapy.[21] Given that O^2-phosphorylation of diazeniumdiolates have not yet been reported, we first designed, synthesized and biologically evaluated a new class of phosphorodiamidate mustard-based O^2-phosphorylated diazeniumdiolates **6–9**. These compounds showed potent anticancer activity. Among them, 7 was the most potent in inhibiting proliferation of six cancer cell lines, especially against MCF-7, superior to JS-K. Interestingly, 7 exhibited selective antiproliferative activity against MCF-7 cells relative to the normal breast epithelial MCF10A cells. Furthermore, 7 released a greater amount of NO and caused more DNA damage and apoptosis than JS-K in MCF-7 cells. Our findings suggest that 7 might be a potential anticancer agent, and this O^2-phosphorylated diazeniumdiolate may provide a better insight into the design of anticancer drug pertaining to diazeniumdiolate-based NO donors.

Experimental

General information

^{1}H NMR, ^{13}C NMR and ^{31}P NMR spectra were recorded with a Bruker Avance 300 MHz spectrometer at 300 K, using TMS as an internal standard. MS spectra were recorded on a Mariner mass spectrometer (ESI) and high resolution mass spectrometry (HRMS) spectra on an Agilent Technologies LC/MSD TOF instrument. Analytical and preparative TLC was performed on silica gel (200–300 mesh) GF/UV 254 plates, and the chromatograms were visualized under UV light at 254 and 365 nm. All solvents were reagent grade and, when necessary, were purified and dried by standard methods. The purity of all compounds tested was characterized by high resolution mass spectrometry (Agilent Technologies LC/MSD TOF). Individual compounds with a purity of >95% were used for biological experiments. Compounds **10–12** were prepared according to ref. 22–24 (see the experimental procedures for **10**, **11** and **12** in ESI†).

General procedure for the synthesis of 6 and 7

A solution of 3 mmol of intermediate **11** in 20 mL of dry THF was cooled to −28 °C under nitrogen. 3 mmol sodium diazeniumdiolate (**13** or **14**) was added and the reaction mixture was stirred at this temperature for 6–8 h until the starting material was totally consumed as indicated by TLC. The solvent was evaporated and then the crude product was purified by column chromatography [4% (v/v) MeOH–CH_2Cl_2] to give **6** (331 mg, 24% yield, TLC R_f 0.64: 6% (v/v) MeOH–CH_2Cl_2) or 7 (401 mg, 29% yield, TLC R_f 0.59: 6% (v/v) MeOH–CH_2Cl_2).

***O*^{2}-[*N*,*N*,*N*′,*N*′-Tetrakis(2-chloroethyl)phosphorodiamidate]1-(*N*,*N*-diethylamino)diazen-1-ium-1,2-diolate (6).**

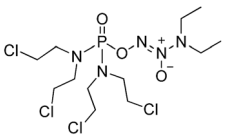

6

The title compound was obtained in 24% yield as a yellow oil. ^{1}H NMR (300 MHz, CD_3OD), δ (ppm): 1.21 (t, $J = 9.0$ Hz, 6H, 2 × CH_3), 3.43–3.71 (m, 12H, 3 × CH_2NCH_2), 3.78–3.83 (m, 8H, 4 × Cl $\underline{CH_2}$ CH_2N). ^{13}C NMR (75 MHz, CD_3OD), δ (ppm): 49.0, 46.5, 41.3, 10.4. ^{31}P NMR (121.5 MHz, CD_3OD), δ (ppm): 17.7. ESI-MS 482.0 $[M + Na]^+$; HRMS calculated for $C_{12}H_{26}Cl_4N_5O_3PNa$ $[M + Na]^+$ 482.0425, found 482.0414 (PPM error of −2.3).

***O*^{2}-[*N*,*N*,*N*′,*N*′-Tetrakis(2-chloroethyl)phosphorodiamidate]1-morpholine-diazen-1-ium-1,2-diolate (7).**

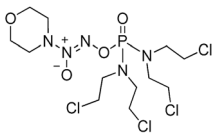

7

The title compound was obtained in 29% yield as a colorless oil. ^{1}H NMR (300 MHz, CD_3OD), δ (ppm): 3.47–3.58 (m, 12H, 3 × CH_2NCH_2), 3.72–3.76 (m, 8H, 4 × Cl $\underline{CH_2}$ CH_2N), 3.84 (t, J = 11.8 Hz, 4H, CH_2OCH_2). ^{13}C NMR (75 MHz, CD_3OD), δ (ppm): 66.5, 52.3, 50.4, 42.8. ^{31}P NMR (121.5 MHz, CD_3OD), δ (ppm): 18.1. ESI-MS 496.0 $[M + Na]^+$; HRMS calculated for $C_{12}H_{24}Cl_4N_5O_4PNa$ $[M + Na]^+$ 496.0218, found 496.0226 (PPM error of 1.6).

General procedure for the synthesis of 8 and 9

A solution of 3 mmol of intermediate **12** in 20 mL of dry THF was cooled to −28 °C under nitrogen. 3 mmol of diazeniumdiolate (**13** or **14**) was added and the reaction mixture was stirred at this temperature for 6–8 h until the starting material was totally consumed as indicated by TLC. The solvent was evaporated and then the crude product was purified by column chromatography [4% (v/v) MeOH–CH_2Cl_2] to give **8** (264 mg, 21% yield, TLC R_f 0.52: 6% (v/v) MeOH–CH_2Cl_2) or **9** (351 mg, 27% yield, TLC R_f 0.47: 6% (v/v) MeOH–CH_2Cl_2).

***O*²-[*N*,*N*-Bis(2-chloroethyl)-*N*′-methylpiperazinyl-phosphorodiamidate]1-[*N*,*N*-diethylamino]diazen-1-ium-1,2-diolate (8).**

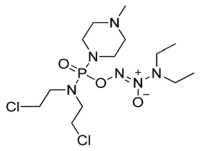

8

The title compound was obtained in 21% yield as a yellow oil. ^{1}H NMR (300 MHz, CD_3OD), δ (ppm): 1.17 (t, J = 5.2 Hz, 6H, 2 × CH_3), 2.33 (s, 3H, CH_3), 2.49 (t, J = 3.0 Hz, 4H, 2 × CH_2), 3.28–3.35 (m, 4H, CH_2NCH_2), 3.42–3.54 (m, 8H, 2 × NCH_2), 3.69–3.74 (m, 4H, 2 × CH_2Cl). ^{13}C NMR (75 MHz, CD_3OD), δ (ppm): 54.4, 49.0, 46.7, 44.9, 44.0, 41.4, 10.6. ^{31}P NMR (121.5 MHz, CD_3OD), δ (ppm): 16.6. ESI-MS 419.2 $[M + H]^+$; HRMS calculated for $C_{13}H_{30}Cl_2N_6O_3P$ $[M + H]^+$ 419.1494, found 419.1501 (PPM error of 1.7).

***O*²-[*N*,*N*-Bis(2-chloroethyl)-*N*′-methylpiperazinyl-phosphoro diamidate]1-morpholine-diazen-1-ium-1,2-diolate (9).**

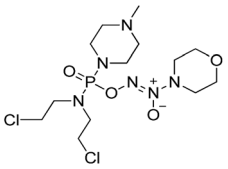

9

The title compound was obtained in 27% yield as a colorless oil. ^{1}H NMR (500 MHz, CD_3OD), δ (ppm): 2.37 (s, 3H, N–CH_3), 2.53–2.59 (m, 4H, 2 × –NCH_2), 3.31–3.34 (m, 4H, 2 × -$PNCH_2$), 3.44–3.50 (m, 4H, 2 × CH_2, chloroethyl), 3.56 (t, J = 4.5 Hz, 4H, CH_2NCH_2, morpholine), 3.71–3.73 (m, 4H, 2 × CH_2Cl, chloroethyl), 3.84 (t, J = 4.8 Hz, 4H, CH_2OCH_2, morpholine). ^{13}C NMR (75 MHz, CD_3OD), δ (ppm): 67.0, 56.3, 52.8, 50.3, 46.6, 45.8, 43.3. ^{31}P NMR (121.5 MHz, CD_3OD), δ (ppm): 16.9. ESI-MS 455.1 $[M + Na]^+$; HRMS calculated for $C_{13}H_{27}Cl_2N_6O_4PNa$ $[M + Na]^+$ 455.1106, found 455.1098 (PPM error of −1.8).

MTT assay

The inhibitory effects on cell proliferation of tested compounds were investigated by the MTT method. All cells were obtained from BIORN Life Science Co. Ltd. Several final density of 1.0 × 10^4 cells per well were placed in 96-well cell plates overnight and treated with or without different concentrations of tested compounds for various periods of time. During the last 4 h culture, the cells were exposed to MTT (5 mg mL^{-1}), and the resulting formazan crystals were dissolved in 150 μL of DMSO and measured using a spectrophotometer (Tecan) at a test wavelength of 570 nm. Experiments were conducted in triplicate. Inhibition rate (%) = $[(A_{control} - A_{treated})/A_{control}] \times 100\%$.

NO release measurement in MCF-7 cells

DAF-FM DA assay. DAF-FM DA (Beyotime) was used as a fluorescent indicator of intracellular NO. When cells grown in a 96-well plate reached 80% confluence, they were washed with PBS. After being loaded with 5 μM DAF-FM DA at 37 °C for 20 min, the cells were rinsed three times with PBS and incubated with test compounds for 8 h. NO production was measured with the flow cytometer with excitation and emission wavelengths of 495 and 515 nm, respectively.

Griess assay. The levels of nitrite were determined by the colorimetric assay using the nitrite colorimetric assay kit (Beyotime, Nanjing, China). Briefly, MCF-7 cells were treated with the indicated concentrations of test compounds, and the nitrite contents of the cell lysates were detected by the Griess assay. The absorbance was read at 540 nm on a spectrophotometer (Smart spec, Bio-Rad). The amount of nitrite in the lysates was calculated using a $NaNO_2$ standard curve in accordance with the manufacturer's instructions (Beyotime).

Comet assay

General. MCF-7 cells were planked in a 48 well plate with a concentration of 10^5 cells per well and cultured in 37 °C 5% CO_2 for 24 h. Then cells were treated with JS-K (10 nM, 100 nM, 1000 nM), **10** (10 nM, 100 nM, 1000 nM) containing EMEM for 2 h. A single cell suspension was obtained from enzymatic dissociation at 37 °C for 30 min using 2 mL 0.25% trypsin and 0.02% EDTA mixed digestive juice. Washed in cold phosphate-buffered saline (PBS) (180g × 5 min, 4 °C) two times by centrifugation and resuspended in fresh cold PBS at the same density, cell count will be adjusted to 1 × 10^6 cell per mL, and will be 100 μL.

Preparation of slide. Fully frosted microscope slides were each covered with 85 μL 1% normal melting agarose (NMA) in Ca^{2+} and Mg^{2+} free phosphate-buffered saline (PBS) at 45 °C, immediately covered with a No. 1 coverslip and then kept at 4 °C for 10 min to allow the agarose to solidify. This first layer was used to promote even and firm attachment of the second and third layers. Control cells suspension is mixed with 70 μL of 1% low melting point agarose (LMA) at 37 °C. After gently removing the coverslip the cell suspension is rapidly pipetted onto the first agarose layer, spread using a coverslip and maintained at 4 °C for 10 min. After removal of the coverslip the third layer of 5% LMA (70 μL) at 37 °C is added, spread using a coverslip and allowed to solidify at 4 °C. After removal of the coverslip the slides are immersed in freshly prepared cold lysing solution (2.5 M NaC1, 100 mM Na_2EDTA, 10 mM Tris; pH 10, 1% sodium sarcosinate, with 1% Triton X-100 and 10% DMSO added just before use) for a minimum of 1 h at 4 °C. Overnight treatment in lysis buffer at 4 °C was tolerated but prolonged lysis results in

precipitation of the buffer. The slides were then removed from the lysing solution, drained and placed in a horizontal gel electrophoresis tank side by side, avoiding spaces and with the agarose end facing the anode (8–21 slides can be accommodated depending upon the size of the tank). The tank was filled with fresh electrophoresis buffer (1 mM Na_2EDTA and 300 mM NaOH) to a level approximately 0.25 cm above the slides. The slides were left in the high pH buffer for 20 min to allow unwinding of the DNA before electrophoresis. Electrophores was conducted at room temperature for 20 min at 25 V, adjusted to 300 mA by raising or lowering the buffer level in the tank. After electrophoresis the slides were washed gently to remove alkali and detergents which would interfere with ethidium bromide staining, by placing them on a tray and flooding them slowly with 3* changes of 0.4 M Tris, pH 7.5, each for 5 rain. After neutralization the slides were each stained with 2 mg mL^{-1} ethidium bromide in distilled water and covered with a coverslip. All the steps described were conducted under yellow light, red light or in the dark to prevent additional DNA damage.

Analysis of slides. For ethidium bromide staining observations were made using an epi-fluorescence microscope equipped with an excitation filter of 515–560 nm from a 100 W mercury lamp and a barrier filter of 590 nm. Photomicrographs of single ceils can be taken at 400× magnification using for example Kodak T-Max 400ASA black and white 35 mm film or alternatively measurements can be made using a calibrated scale in the ocular of the microscope. Samples were viewed as soon as possible following staining though preparations can be successfully stored up to a few days in a light proof box containing moist (PBS) sponges at 4 °C, before analysis. DNA migration can be determined on negative photomicrographs using 0–150 mm digital calipers by measuring the nuclear DNA and migrating DNA (*i.e.* comet length (ram)) and head diameter (mm) in a minimum of 25 randomly selected cells per population being studied. Comet area (mm^2) can be measured by placing a mm^2 graph transparency between a light box and the negative and counting the number of squares over which the comet extends. Image analysis equipment was, however, required for comprehensive and large scale comet analysis.

Data analysis. ANOVA one-way and Tukey's test were used in the test data group, and the *P* value less than 0.05 was considered to be significant difference.

Apoptosis analysis. Cells were incubated in six-well plates (1×10^5 per well) and treated with DMSO (1%), **7**, or JS-K for 24 h. To quantify apoptosis, prepared cells were washed twice with cold PBS and then resuspended in 500 μL binding buffer at a concentration of 1×10^6 cells per mL. 5 μL FITC–Annexin-V and 5 μL PI were then added to these cells, which were kept in the dark at 25 °C for 10 min. Data acquisition and analysis were performed in a FACS calibur flow cytometer (Becton Dickinson) and calculated by Cell Quest software (BD Biosciences, Franklin Lakes, NJ).

Acknowledgements

This work was supported by grants from the National Natural Science Foundation of China (No. 21372261 and No. 81673305) and Jiangsu Province Funds for Distinguished Young Scientists (BK20160033). Part of the work was supported by the Priority Academic Program Development of Jiangsu Higher Education Institutions (PAPD), Program for New Century Excellent Talents in University (NCET-13-1033), College Students Innovation Project for the R & D of Novel Drugs (J1030830), and Jiangsu Shuang Chuang team.

Notes and references

1 E. Culotta and D. E. Koshland Jr, *Science*, 1992, **258**, 1862–1865.
2 W. Xu, L. Z. Liu, M. Loizidou, M. Ahmed and I. G. Charles, *Cell Res.*, 2002, **12**, 311–320.
3 B. Oronsky, G. R. Fanger, N. Oronsky, S. Knox and J. Scicinski, *Clin. Transl. Oncol.*, 2014, **7**, 167–173.
4 R. A. Serafim, M. C. Primi, G. H. Trossini and E. I. Ferreira, *Curr. Med. Chem.*, 2012, **19**, 386–405.
5 A. B. Seabra, R. de Lima and M. Calderon, *Curr. Top. Med. Chem.*, 2015, **15**, 298–308.
6 D. Hirst and T. Robson, *J. Pharm. Pharmacol.*, 2007, **59**, 3–13.
7 S. Huerta, S. Chilka and B. Bonavida, *Internet J. Oncol.*, 2008, **33**, 909–927.
8 R. Scatena, P. Bottoni, G. E. Martorana and B. Giardina, *Expert Opin. Invest. Drugs*, 2005, **14**, 835–846.
9 J. E. Saavedra, T. M. Dunams, J. L. Flippenanderson and L. K. Keefer, *J. Org. Chem.*, 1992, **57**, 6134–6138.
10 J. E. Saavedra, P. J. Shami, L. Y. Wang, K. M. Davies, M. N. Booth, M. L. Citro and L. K. Keefer, *J. Med. Chem.*, 2000, **43**, 261–269.
11 R. S. Nandurdikar, A. E. Maciag, S. Y. Hong, H. Chakrapani, M. L. Citro, L. K. Keefer and J. E. Saavedra, *Org. Lett.*, 2010, **12**, 56–59.
12 P. J. Shami, J. E. Saavedra, L. Y. Wang, C. L. Bonifant, B. A. Diwan, S. V. Singh, Y. Gu, S. D. Fox, G. S. Buzard, M. L. Citro, D. J. Waterhouse, K. M. Davies, X. Ji and L. K. Keefer, *Mol. Cancer Ther.*, 2003, **2**, 409–417.
13 A. E. Maciag, H. Chakrapani, J. E. Saavedra, N. L. Morris, R. J. Holland, K. M. Kosak, P. J. Shami, L. M. Anderson and L. K. Keefer, *J. Pharmacol. Exp. Ther.*, 2011, **336**, 313–320.
14 T. Kiziltepe, T. Hideshima, K. Ishitsuka, E. M. Ocio, N. Raje, L. Catley, C. Q. Li, L. J. Trudel, H. Yasui, S. Vallet, J. L. Kutok, D. Chauhan, C. S. Mitsiades, J. E. Saavedra, G. N. Wogan, L. K. Keefer, P. J. Shami and K. C. Anderson, *Blood*, 2007, **110**, 709–718.
15 P. J. Shami, J. E. Saavedra, C. L. Bonifant, J. Chu, V. Udupi, S. Malaviya, B. I. Carr, S. Kar, M. Wang, L. Jia, X. Ji and L. K. Keefer, *J. Med. Chem.*, 2006, **49**, 4356–4366.
16 R. A. D'Sa, Y. Wang, P. H. Ruane, B. M. Showalter, J. E. Saavedra, K. M. Davies, M. L. Citro, M. N. Booth, L. K. Keefer and J. P. Toscano, *J. Org. Chem.*, 2003, **68**, 656–657.
17 D. F. Dourado, P. A. Fernandes, M. J. Ramos and B. Mannervik, *Biochemistry*, 2013, **52**, 8069–8078.
18 H. Kojima, Y. Urano, K. Kikuchi, T. Higuchi, Y. Hirata and T. Nagano, *Angew. Chem., Int. Ed. Engl.*, 1999, **38**, 3209–3212.

19 D. S. Bredt and S. H. Snyder, *Annu. Rev. Biochem.*, 1994, **63**, 175–195.
20 P. J. Shami, D. L. Sauls and J. B. Weinberg, *Leukemia*, 1998, **12**, 1461–1466.
21 L. K. Keefer, *ACS Chem. Biol.*, 2011, **6**, 1147–1155.
22 M. H. Lyttle, A. Satyam, M. D. Hocker, K. E. Bauer, C. G. Caldwell, H. C. Hui, A. S. Morgan, A. Mergia and L. M. Kauvar, *J. Med. Chem.*, 1994, **37**, 1501–1507.
23 A. Satyam, M. D. Hocker, K. A. Kane-Maguire, A. S. Morgan, H. O. Villar and M. H. Lyttle, *J. Med. Chem.*, 1996, **39**, 1736–1747.
24 X. L. Chen, J. W. Yuan, L. B. Qu, Z. B. Qu, S. H. Xu, F. J. Wang and Y. F. Zhao, *Phosphorus, Sulfur Silicon Relat. Elem.*, 2012, **187**, 245–254.